Novel Automated 3D Registration in CT Subtraction Angiography

Peter, R.[1], Malínský M.[1], Jan, J.[1], Ouředníček P.[2]
[1]Brno University of Technology, Dept. of Biomedical Engineering
[2]Philips Medical Systems Nederland, B.V.
xpeter12@stud.feec.vutbr.cz, xmalin09@stud.feec.vutbr.cz, jan@feec.vutbr.cz,
petr.ourednicek@philips.com

Abstract. CT subtraction angiography plays a crucial role in diagnostics and medical treatment, especially in case of peripheral vascular disease [1]. The subtraction process is usually violated due to the patient movement between and during acquisition phases. The main condition for high-quality extraction and visualization of peripheral vessel tree is to reliably remove all bones from the postcontrast acquisition. Our approach of CTA subtraction is based on precise volume registration of corresponding bones obtained from the native and postcontrast acquisition phases. Based on the fact that each individual bone is a rigid body, for the registration of these objects the rigid transform with different parameters for each individual bone is used, but because of the patient movement also during the image acquisition followed by minor flexible post-registration.

1 Introduction

The paper describes a novel method of vessel structure extraction from the 3D CT angiography data. As mentioned in Maksimov et al. [2], there is a reliable approach, which would fully remove all bones without violating the blood vessel tree. The algorithm proposed by Maksimov allows to remove most of the bony structures as well as calcifications using local matching and image processing, nevertheless it has some shortcomings in the case where arteries are near to bones. To solve this problem, better non-rigid strategies have to be determined.

Our approach is based on a combination of rigid and non-rigid volume registration of corresponding bones segmented from the pre-contrast and post-contrast image data. For the surrounding soft tissue elimination, the rigid transform parameters derived for nearest neighbouring bones are used. The final subtracted volume data is then created from a number of subtracted parts, derived as mentioned above.

2 Methods

In order to eliminate vessel distortion we use the post-contrast image data as the reference image in the process of registration. Based on the fact that each individual bone is a rigid body, for the registration of these objects rigid transforms are used (albeit with generally different parameters for each individual bone). For the application of the individual rigid transforms of the bone data, the bones must be segmented out reliably.

2.1 Preprocessing

To define the area of interest and eliminate all redundant objects like patient desk and quantum noise artefacts, some heuristics utilising morphological approaches are used [3]. Bones are segmented by threshold defined from parameters (combination of mean values) of two Gaussian curves derived by approximating of histogram [4, 5]. For each bone from pre-contrast phase the corresponding bone from post-contrast phase is searched. Correspondences between both acquisition phases are evaluated as reliable or unreliable.

As for this reliability, bone-lockers (dilated areas of segmented bones, Fig 1.) are created either from post-contrast images for reliable bones or from pre-contrast images. The reason is to eliminate the case, where bones in postcontrast phase image are connected.
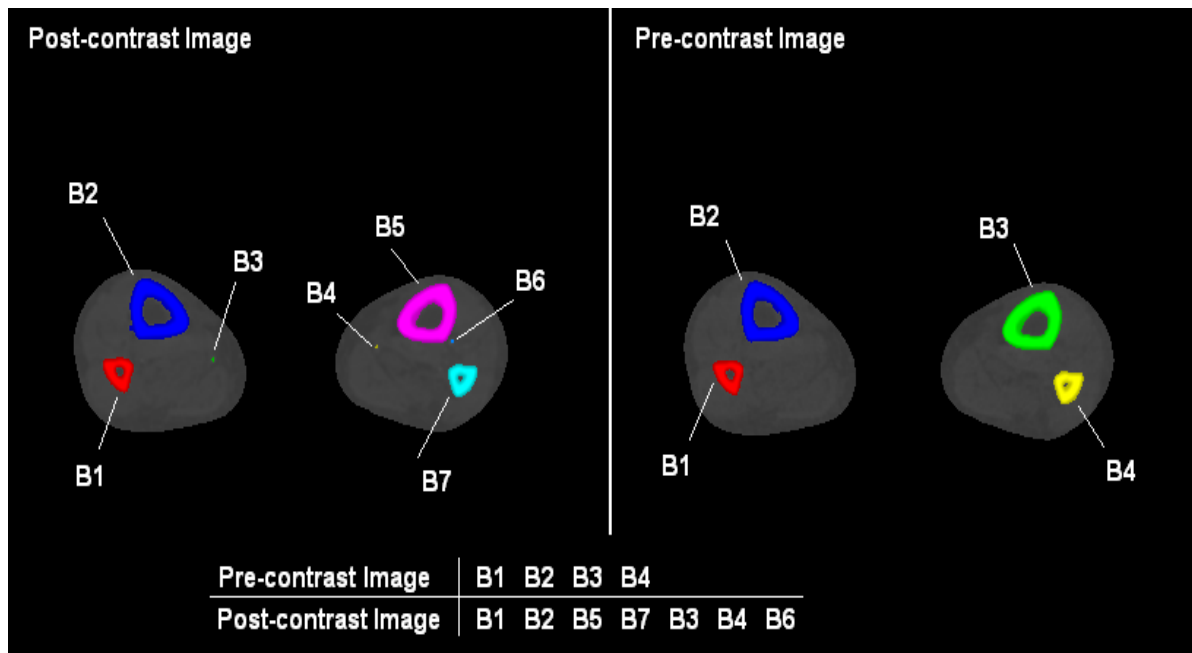

Fig 1.Segmented and assigned high-density objects

2.2 Registration

In case of rigid registration we use a stochastic optimisation method called Controlled Random Search, which is based on evolution strategy. As mentioned in [6], the main advantage of this method is that there are more vectors of parameters defining an initial population and also the possibility to use different heuristics for searching of the optimal solution. The similarity is evaluated using the angle (cosine) criterion (1) [7]

$$C_A(\bar{x}, \bar{y}) = \frac{\bar{x}\,\bar{y}}{|\bar{x}| \cdot |\bar{y}|} = \frac{\sum_{i=1}^{N} x_i\, y_i}{\sqrt{\sum_{i=1}^{N} x_i^2 \cdot \sum_{i=1}^{N} y_i^2}},\tag{1}$$

where $\bar{x} = \{x_1...x_n\}$ and $\bar{y} = \{y_1...y_n\}$ represent the vectors of both image intensities.

Unfortunately, due to possible patient movements during the image acquisition, a flexible post-registration for each bone is needed. The locally defined transforms are derived based on disparity maps. To obtain the disparity map, we use the non-parametric diffusion method called Demon [8, 9], which is physically based on the optical-flow. Due to the iterative concept of this method, displacements u (both pixel and sub-pixel values) are determined:

$$u = \frac{(m-f)\nabla f}{|\nabla f|^2 + \alpha^2 (m-f)^2} + \frac{(m-f)\nabla m}{|\nabla m|^2 + \alpha^2 (m-f)^2}$$

where $\mathbf{u} = (u_x, u_y, u_z)$ represents the 3D displacement field, $\mathbf{f}$ is the intensity of static image, $\mathbf{m}$ is the intensity of floating image, α is estimated noise constant and $\nabla \mathbf{f}$ is gradient of static image. This way defined registration process ensures reliable elimination of bones.

2.3   Subtraction

There are two classes of subtracted data obtained as follows. Data A contain the data from subtraction of each individual bone. Using the rigid parameters of each bone a number of geometrically transformed native data are created and subtracted from the original postcontrast image. This provides B_1-B_N subtractions, Fig. 2.
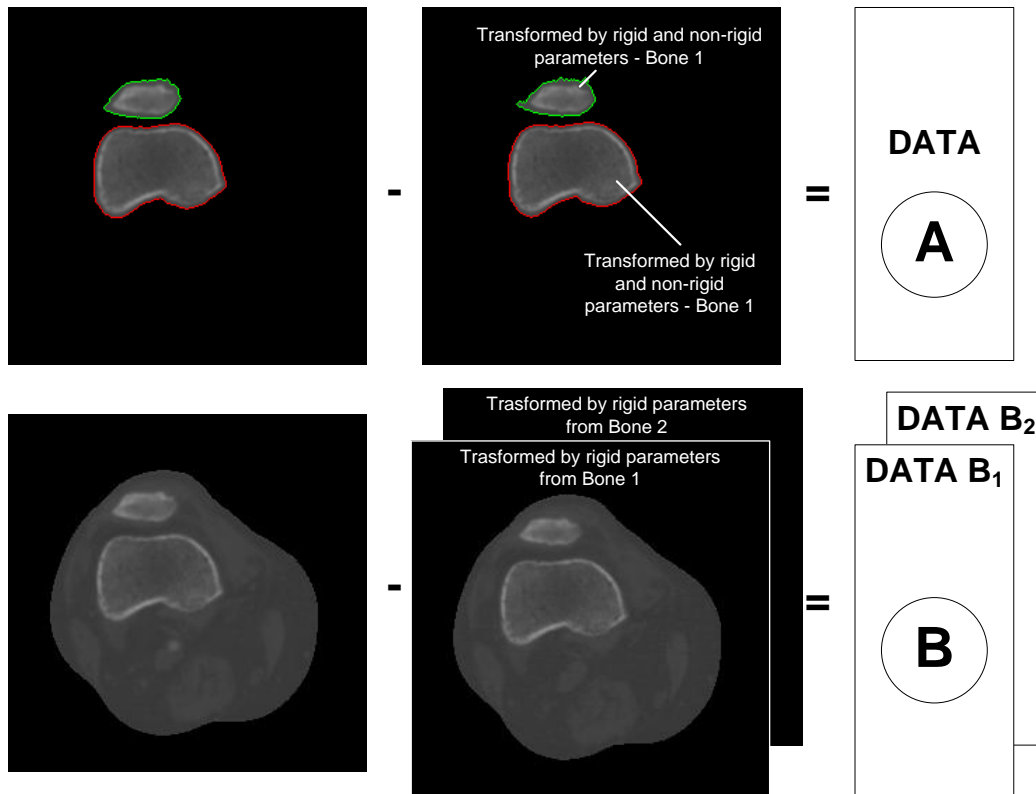
Fig 2.Subtraction process

Because we presume that the intensity of contrast vessel is always higher than the soft tissue in native image, it is possible to merge the final subtraction as shown on Fig. 3. The white areas are defined using the bone-lockers mentioned in chapter 2.1 and represented by values of data A, while the grey areas are represented by minimal values from subtractions B_1-B_N with respect to the position.
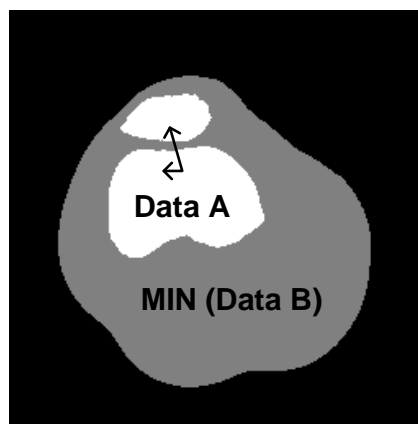
Fig 3.Merging process

3   Conclusions

Using this approach, we are presently able to provide rather good 3D vessel visualisation without important traces of other tissues (Fig.4), generally providing higher detail than standard programs. In the radiologist view, these results enable to trace clearly more detailed vessel structure compared to images provided by standard commercial software belonging to the CT imaging system. As it can be seen, some artefacts still remain, probably due to imperfect matching of neighbouring sections of data; this is presently under further research.

Fig 4.MIP visualization - comercial system (left), proposed method (right)

Acknowledgement

References

[1] LIN et al.: Assessment of Aortic Pathology and Peripheral Arterial Disease Using Multidetector Computed Tomographic Angiography, *Vasc Endovascular Surg.*2009; 42: 583-598

[2] MAKSIMOV, D., FINKEL, F., DIETZ, T., DIEHL, S.D.C, REBHOLZ, P., HESSER, J., MANNER, R: An Interactive Application for Removal of Bone Information in CT-Angiography, *17th Computer-Based Medical Systems IEEE Symposium on*, p. 396, 2004

[3] JAN, J. Medical Image Processing, Reconstruction and Restoration - Concepts and Methods. Boca Raton, FL, USA: CRC Press, Taylor and Francis Group, 2005. 760 s. ISBN: 0-8247-5849-8.

[4] WANG, L., GREENSPAN, M., ELLIS, R.: Validation of Bone Segmentation and Improved 3-D Registration Using Contour Coherency in CT Data. *IEEE Trans Med Imaging*. 2006 Mar; 25(3):324-34. PMID: 16524088.

[5] YAN, K., ENGELKE, K., KALENDER, W. A.: A New Accurate and Precise 3-D Segmentation Method for Skeletal Structures in Volumetric CT Data, *Medical Imaging, IEEE Transactions on*, vol. 22, no.5, pp.586-598, May 2003

[6] TVRDIK, J.: Differential Evolution: Competitive Setting of Control Parameters, *Proceedings International Multiconference on Computer Science and Information Technology*, Wisla, Poland, 2006, 207 - 213.

[7] JAN, J., JANOVA, D.: Complex Approach to Surface Reconstruction of Microscopic Samples from Bimodal Image Stereo Data. *Mach. Graphics Vision*, 10, 2001, pp. 261-288 (special issue on stereogrammetry and related topics).

[8] THIRION, J.P.: Image Matching as a Diffusion Process: An Analogy With Maxwell's Demons, *Medical Image Analysis*, pp. 243–260, 1998.

[9] KROON, D.-J., SLUMP, C.H.: MRI Modality Transformation in Demon Registration, *IEEE International Symposium on*, pp. 963-966, Boston MA, July 1 2009, ISBN: 978-1-4244-3931-7.